TECHNICAL MEMORANDUMS

NATIONAL ADVISORY COMMITTEE FOR AERONAUTICS

No. 889

INVESTIGATION OF THE LIFT DISTRIBUTION OVER THE SEPARATE WINGS OF A BIPLANE

By D. Küchemann

Luftfahrtforschung
Vol. 15, No. 10/11, October 10, 1938
Verlag von R. Oldenbourg, München und Berlin

Washington
March 1939

NATIONAL ADVISORY COMMITTEE FOR AERONAUTICS

TECHNICAL MEMORANDUM NO. 889

INVESTIGATION OF THE LIFT DISTRIBUTION OVER THE SEPARATE WINGS OF A BIPLANE*

By D. Küchemann

An investigation is made of the mutual interference of the wings of a biplane under the general assumption that each wing may be replaced by a vortex system of the type given by the Prandtl wing theory. The additional velocities induced at each wing by the presence of the other are determined by the Biot-Savart law and converted into an equivalent change in angle of attack, the effect being that of an additional twist given to the wings in changing their lift distributions. The lift distributions computed in this manner for several airplane types are compared with the results of measurement.

Notation

In general the subscript o will denote the value for the upper wing, whereas the subscript u will denote the corresponding value for the lower wing;

x, y, z, rectangular coordinates (right-hand system); the y axis laid in the direction of the bound or lifting vortex of the lower wing positive to starboard, origin taken at the center of the wing, and the x axis forward

a, stagger of the biplane system = separation of lifting vortices in the x direction

h, wing gap = separation of lifting vortices in the z direction

t, wing chord

b, wing span

*"Berechnung der Auftriebsverteilung über die einzelnen Flügel eines Doppeldeckers." Luftfahrtforschung, Oct. 10, 1938, pp. 543-55.

$\eta = 2y/b$, nondimensional coordinate in the y direction

α and α_g, angle of attack measured from the zero lift direction of the upper wing

α_i, self-induced angle of attack

$\alpha_{i_{ou}}$, angle of attack induced at the upper wing by the presence of the lower wing

$\alpha_{i_{uo}}$, correspondingly for the lower wing

α_e, effective angle of attack

f_e, effective rise of camber

V, undisturbed velocity at infinity

u, w, induced velocity components in the x and y directions, respectively

A, W, M, lift, drag, and moment per unit length

$c_a = \frac{A}{\frac{\rho}{2} v^2 t}$, section lift coefficient

$c_w = \frac{W}{\frac{\rho}{2} v^2 t}$, section drag coefficient

$c_m = \frac{M}{\frac{\rho}{2} v^2 t^2}$, section moment coefficient

$\overline{c_a} = \frac{\overline{A}}{\frac{\rho}{2} V^2 F}$, total lift coefficient of a wing

$\overline{c_{a_d}}$, total lift coefficient of cellule referred to the total area.

Γ, circulation

$\gamma = \frac{\Gamma}{b\ V} = \frac{c_a\ t}{2\ b}$, nondimensional coefficient of the circulation

$\Lambda = b^2/F$, aspect ratio of a wing

$c_1 = \frac{1}{2}\left(\frac{d\ c_a}{d\ \alpha}\right)_{\Lambda \longrightarrow \infty}$, lift slope

I. REVIEW OF PREVIOUS WORK DONE ON THE BIPLANE PROBLEM

The solution of the monoplane wing problem having been obtained, that of the biplane lifting system consisting of the combination of two airfoils presents new problems for the airfoil theory to solve, because of the fact that each wing is located in the disturbed flow produced by the other. Each wing of the cellule therefore exerts an essential influence on the position and magnitude of the aerodynamic forces on the other. From the practical viewpoint, an answer is required to the following two questions:

1. How large is the total lift of each of the wings and of the biplane combination?

2. How is the lift distributed over the span of each wing?

In connection with the second question, a third one arises, namely,

3. What lift distribution gives the minimum induced drag of the lifting system?

The first question has already received the attention of a large number of investigators, whereas an attempt to answer the second will be the object of the present paper. To the third questions a general solution had already been found very early in the development of the theory.

I should like first to give a brief review of the work that has so far been done on the biplane problem. This work is almost entirely concerned with the answer to the first question. It is convenient to distinguish two groups of theoretical investigations. A first group considers wings of finite span (three-dimensional problem). In those investigations in which only the total lift is to be determined, assumptions are made on the lift distribution so that each wing is replaced either by a horseshoe vortex or by a vortex system with elliptic lift distribution. It is then possible to consider theoretically the mutual interference of such vortex systems. The finite chord of the airfoil is only approximately taken into consideration. In contrast to this group there is a second

larger group of investigations, which takes the effect of the finite chord into account by considering the two dimensional flow, but which does not take into account the effect of the finite span or only estimates it. This second mode of treatment has the advantage over the first in that the mathematical aids of conformal transformation and integral equations are to a large extent made available and this also explains the large number of these investigations. The method has the disadvantage that the effect of the chord, which is mainly taken into account, is in general considerably smaller than the effect of the finite span of the wings. We shall first consider the group of investigations, which deals the solution of the first problem, namely, that which takes the three-dimensional problem as the starting point.

The first computation of the mutual intereference effect of two airfoils which led to practical formulas is due to A. Betz (references 1 and 2). The general method of treatment is essentially the same as that given in the present paper and will be presented in detail below. As a basis, the assumption was made that the lift is uniformly distributed over the span (simple horseshoe vortex). It was possible in this way to determine the change in total lift to a first approximation. A refinement of the method by L. Prandtl (references 3 and 4) assumes elliptic distribution for both wings. The carrying through of the computation was in this case, however, made considerably more difficult so that only simpler problems than those considered by A. Betz could be solved. In connection with this, H. von Sanden (reference 5) gave a numerical computaion of the deviation in the obtained mean downwash velocity induced by the trailing vortices as given by the theory when uniform and elliptic lift distributions, respectively, were assumed. There was obtained the oft-mentioned result that the differences in those mean values that are of importance for the total lift and drag are not usually very large. An attempt was made later to take greater account of the wing chord. The due consideration of the wing chord is, as we shall see later, important for the reason that not only is the velocity at one wing changed by the presence of the other but also the streamlines in the neighborhood receive a curvature. N. K. Bose (reference 6) has particularly investigated the effect of curvature of the streamlines. A comparison of his results with those obtained for the streamline curvature in the present paper showed good agreement. A comprehensive presentation of this method of treating the biplane problem has been found by R. Fuchs (reference 7), who has developed and refined

the method in a paper as yet unpublished, so that the total lift may be determined by this method with sufficient accuracy in most of the practical cases occurring. This essentially completes the list of the first group of papers which concerns itself directly with the three-dimensional problem. All these theories are based on particular assumptions on the lift distributions over the two wings and compute the change in the total lift.

A brief reference may be made here to the papers which deal with the answer to the third question and which are also concerned with the three-dimensional flow about the biplane cellule. These are the papers by L. Prandtl (references 3 and 4) and by M. M. Munk (reference 8) in which is determined the lift distribution which gives the minimum induced drag of the biplane cellule. These papers also contain general theorems on the induced drag of biplane lifting systems.

Again returning to the reports that have appeared on the solution of the first of the above-mentioned problems, we come to that group in which the problem is reduced to a two-dimensional one. It is not possible here to give a detailed account of all the methods used. Essentially the two-dimensional flow about two infinite airfoils was investigated with the aid of the theory of conformal transformation or that of integral equations. The first investigation of this kind with reference to practical application is that of W. M. Kutta (reference 9), whose investigation was again carried out more in detail by R. Grammel (reference 10). In the papers by E. Pohlhausen (reference 11), M. M. Munk (reference 12), B. Eck (reference 13), T. Moriya (reference 14), H. Glauert (reference 15), M. Lagally (reference 16), C. B. Millikan (reference 17), I. Tani (reference 18), C. Ferrari (reference 19), E. Pistolesi (reference 20), G. Schmitz (reference 21), P. Teofilato (reference 22), J. Bonder (reference 23), P. Koebe (reference 24), I. E. Garrick (reference 25), and E. Graeser (26), there is treated principally the conformal transformation of two circular arcs into profiles, and conclusions are then derived for the biplane. The amount of computation for specified profile shapes is, however, quite considerable. In some of the papers the very important effect of the trailing vortices (see computation under section III) is sufficiently well taken into account. B. Eck (reference 13) replaces, for example, the effect of the trailing vortices by a uniform downwash velocity and thus the flow about the biplane by a two-dimensional flow, a mean circulation, and an

elliptic lift distribution being assumed for both wings. In various French papers the results of the two dimensional theory are given and partly extended to the three-dimensional cases. A comprehensive report covering this work by M. Nenadovitch will be found in reference 27. He also conducted a large number of measurements on approximately two-dimensional flows. This practically completes the list of theoretical investigations.

The theoretical papers are supplemented by a number of experimental papers. In addition to the above-mentioned French measurements (reference 27), there are those of M. M. Munk (references 28 and 37); also, a large number of English measurements of which we may mention those of W. L. Cowley and H. Levy (reference 29), W. L. Cowley and C. N. H. Lock (reference 30), and W. L. Cowley and L. Jones (reference 31) (some further though not so detailed measurements are found in the British A.R.C. Reports and Memoranda); further, the results of the Aerodynamic Experimental Institute of Göttingen (reference 32) and those of F. H. Norton (reference 33), a quite comprehensive series of measurements by the Toronto University, Canada (references 34, 35, and 36) in which are included also pressure distribution measurements; and finally the tests of A. I. Fairbanks (reference 38), O. E. Loeser (reference 39), M. Knight and R. W. Noyes (references 40 and 41), and H. A. Pearson (reference 42). Some of these measurements will be used for checking our results. Unfortunately, measurements of a kind that will satisfy all requirements and from which the lift distributions over the wing spans may be obtained exist only in very small number, so that a systematic test program including pressure distribution measurements in a large wind tunnel would be very desirable.

In conclusions reference may be made to a group of papers which are concerned with the development of working charts for practical application, utilizing the theoretical and experimental results available. Of chief importance are those of P. Kuhn (reference 43) and W. S. Diehl (reference 45). In these a knowledge of the total lift of the cellule is assumed and this lift is then distributed between the upper and lower wing. A determination of this kind can be only very rough since the parameters of stagger, gap, span, chord, lift slope, angle of attack, and decalage, as we shall see below, do not always enter linearly. A comparison of our results with those of W. S. Diehl (references 44 and 45) indicated the possibility of making the results of the latter agree accurately with ours.

II. STATEMENT OF THE PROBLEM

In the present report an attempt will be made to answer the second of the above-mentioned questions (section I). We shall therefore consider a biplane of finite span and try to compute the lift distribution over each wing for a given shape of the biplane cellule. The exact distribution is important for the static computation of the cellule and for the computation of the field of flow about the wings, particularly for the downwash at the tail, and finally, for the determination of those positions along the span at which with increasing angle of attack the maximum lift coefficient $c_{a_{max}}$ is first attained.

For the main portion of the computation we shall replace each of the airfoils by a straight lifting vortex filament with variable circulation as is done in the Prandtl theory for the monoplane (fig. 1). The lifting line will be passed through the center of the profile section. It will, however, appear below that, particularly for small gaps and in the range near the zero angle of attack, this simple assumption will not suffice and it will be necessary to replace each wing by at least two vortex filaments. How this is to be done will be shown more in detail later, section V. This substitution takes account of the finite chord of the wing. We also take into consideration the wing chord in all cases in the determination of the effect of the streamline curvature.

We shall first determine the mutual interference of the two wings of the biplane. The vortex system of the lower wing induces at the location of the upper wing additional velocities which may be converted into a change in the angle of attack of the upper wing, and conversely. This is equivalent to a twist given to each wing by the presence of the other. With the aid of this additional angle of attack, which we shall denote as "externally induced," and the self-induced angle of attack, we can then compute the effective angle of attack from the geometrical:

$$\alpha_{e_o} = \alpha_o - \alpha_{i_o} - \alpha_{i_{ou}} \tag{1}$$

$$\alpha_{e_u} = \alpha_u - \alpha_{i_u} - \alpha_{i_{ou}} \tag{2}$$

The subscripts o and u will denote respectively the upper and lower wings, so that, for example, $\alpha_{i_{ou}}$ is the angle of attack of the upper wing induced by the presence of the lower. With the aid of these equations, the two problems set up by L. Prandtl for the monoplane can be solved for the case of the biplane. The first problem, namely, to determine the wing shape for a given lift distribution, offers no difficulties. In this paper we shall consider the practically more important problem, namely, for a given biplane cellule to compute the lift distribution over each wing. We must first determine the externally induced or interference angles of attack $\alpha_{i_{ou}}$ and $\alpha_{i_{ue}}$ as functions of the shape of the biplane cellule and the angles of attack of each wing.

III. DETERMINATION OF THE INTERFERENCE ANGLES OF ATTACK AND THE SETTING UP OF THE GENERAL EQUATIONS FOR THE CIRCULATIONS

The interference angles of attack $\alpha_{i_{ou}}$ and $\alpha_{i_{uo}}$ result from the combined effect of many factors, which will now be considered. In general, we determine according to the Biot-Savart law the velocities induced at the midpoints of the wing sections of one wing by the vortex elements of the other and convert the x and z components u and w, respectively, in the usual manner into an increment in the angle of attack.

The bound or lifting vortex of each wing induces at the location of the other wing a change in angle of attack:

1. Through a change in the undisturbed longitudinal velocity (x component)

2. Through an additional upwash or downwash component (z component)

3. Through curvature of the streamlines as a result of the change in w with x.

The trailing vortices induce at the wing a change in angle of attack:

1. Through additional upwash or downwash velocities (z component)

2. Through curvature in the streamlines due to change of w with x.

We first consider the upper wing (fig. 2). The detailed computation of the velocity components according to the Biot-Savart law may be dispensed with here (see for example, Glauert (reference 15)). We need only consider somewhat more closely the conversion into angle of attack, the effect of the change in the undisturbed longitudinal velocity, and the curvature effect.

In order to determine the first, we start with the Prandtl airfoil equation for the monoplane,* which may, for example, be the upper wing alone:

$$\frac{\Gamma_o}{c_{l_o} V_o t_o} = \alpha_o - \frac{1}{4\pi V_o} \int_{-\frac{b_o}{2}}^{+\frac{b_o}{2}} \frac{d\Gamma_o}{dy_o'} \frac{dy_o'}{y_o - y_o'} \qquad (3)$$

and assume that

$$V_o = V + \Delta V = V\left(1 + \frac{\Delta V}{V}\right)$$

where V is the undisturbed velocity and ΔV its increment, that is, the x component of the velocity induced by the lifting vortex of the lower wing at the upper wing. Equation (3) thus becomes on multiplication by $(1 + \Delta V/V)$:

$$\frac{\Gamma_o}{c_{l_o} V t_o} = \alpha_o + \alpha_o \frac{\Delta V}{V} - \frac{1}{4\pi V} \int_{-\frac{b_o}{2}}^{+\frac{b_o}{2}} \frac{d\Gamma_o}{dy_o'} \frac{dy_o'}{y_o - y_o'}$$

The velocity increment ΔV thus corresponds to a change in the angle of attack

---

*It is assumed that the flow is potential.

$$\Delta \alpha_o = \alpha_o \frac{\Delta V}{V}$$

(see fig. 4).

The curvature of the streamlines due to the lifting vortex of the lower wing gives rise to an angle of attack increment (see, for example, Glauert, reference 15)

$$\Delta \alpha_o = \frac{t_o}{4 R_o} = \frac{t_o}{4} \frac{\partial}{\partial x} \left(\frac{w_{o_z}}{V_o} \right)$$

where R_o is the radius of curvature of the streamlines and w_{o_z} the z component of the velocity induced at the upper wing by the lifting and trailing vortices of the lower wing. The equation is based on the practically adequate assumption (see, for example, Pistolesi, reference 46) that a plane wing in a flow concave downward possesses the same lift as a wing convex downward possesses in an uncurved flow. Limiting ourselves to the linear members in the disturbance velocities, we obtain

$$\Delta \alpha_o = \frac{t_o}{4 V} \frac{\partial w_{o_z}}{\partial x}$$

It is of interest to compare the curvature effect obtained if in w_{o_z} only the effect of the lifting vortex is taken into account and if also that of the trailing vortex is considered. The result appears in all the computed examples which include the normal range of stagger-gap ratio a/h that the effect of the lifting vortex on the curvature of the streamlines is greater by far than that of the trailing vortex (fig. 6). It can thus be understood why the previously carried out computations of the curvature effect for two-dimensional flow where only the influence of the lifting vortex was taken into account gave relatively good results. All the above considerations may correspondingly be applied to the lower wing (fig. 3).

Before writing down the equations for computing the circulation, we shall introduce a few more brief notations:

$$\sqrt{a^2 + h^2 + \left(\frac{b_u}{2}\eta_u' - \frac{b_o}{2}\eta_o\right)^2} = f_{1_o}$$

$$\sqrt{h^2 + \left(\frac{b_u}{2}\eta_u' - \frac{b_o}{2}\eta_o\right)^2} = f_{2_o}$$

$$h^2 - \left(\frac{b_u}{2}\eta_u' - \frac{b_o}{2}\eta_o\right)^2 = f_{3_o}$$

for the upper wing, and

$$\sqrt{a^2 + h^2 + \left(\frac{b_o}{2}\eta_o' - \frac{b_u}{2}\eta_u\right)^2} = f_{1_u}$$

$$\sqrt{h^2 + \left(\frac{b_o}{2}\eta_o' - \frac{b_u}{2}\eta_u\right)^2} = f_{2_u}$$

$$h^2 - \left(\frac{b_o}{2}\eta_o' - \frac{b_u}{2}\eta_u\right)^2 = f_{3_u}$$

for the lower wing.

As may be easily seen f_{1_o}, f_{2_o}, and f_{1_u}, f_{2_u} represent geometrical distances (see figs. 2 and 3), which may be read off from a drawing of the cellule and thus the computation simplified. The terms f_{3_o} and f_{3_u}, respectively, were obtained by the combination of other expressions.

Combining, we obtain from (1) and (2) after some transformations for the circulation distribution of the upper wing:

$$\left.\begin{aligned}\frac{\gamma_o b_o}{c_{l_o} t_o} &= \alpha_o - \frac{1}{2\pi}\int_{-1}^{+1} \frac{d\gamma_o}{d\eta_o'}\frac{d\eta_o'}{\eta_o' - \eta_o} \qquad \text{(monoplane equation)}\\ &+ \frac{b_u^2}{8\pi}\left[\alpha_o h \int_{-1}^{+1} \gamma_u \frac{d\eta_u'}{f_{1_o}^3}\right. \qquad \text{(change in longitudinal velocity)}\\ &+ a\int_{-1}^{+1} \gamma_u \frac{d\eta_u'}{f_{1_o}^3} \qquad \text{(downwash due to lifting vortex)}\\ &- \int_{-1}^{+1} \gamma_u \left\{\frac{f_{3_o}}{f_{2_o}^4} - a\,\frac{f_{3_o}(a^2+h^2) - 2\left(\frac{b_u}{2}\eta_u' - \frac{b_o}{2}\eta_o\right)^4}{f_{1_o}^3 f_{2_o}^4}\right\} d\eta_u'\\ &\qquad \text{(downwash due to trailing vortex)}\\ &+ \left.\frac{t_o}{4}\int_{-1}^{+1} \gamma_u \left\{\frac{1}{f_{1_o}^3} - \frac{3h^2}{f_{1_o}^5}\right\} d\eta_u'\right] \qquad \text{(curvature effect)}\end{aligned}\right\} \quad (4)$$

where $\gamma = \Gamma/bV$.

For the lower wing we obtain from equation (2):

$$\left.\begin{aligned}
\frac{\gamma_u\, b_u}{c_{l_u}\, t_u} &= \alpha_u - \frac{1}{2\pi}\int_{-1}^{+1} \frac{d\,\gamma_u}{d\,\eta_u'}\,\frac{d\,\eta_u'}{\eta_u' - \eta_u} \qquad \text{(monoplane equation)} \\
&+ \frac{b_o^{\,2}}{8\pi}\left[- \alpha_u h \int_{-1}^{+1} \gamma_o \frac{d\,\eta_o'}{f_{1_u}^{\,3}} \qquad \text{(change in longitudinal velocity)}\right. \\
&- a\int_{-1}^{+1} \gamma_o \frac{d\,\eta_o'}{f_{1_u}^{\,3}} \qquad \text{(downwash due to lifting vortex)} \\
&- \int_{-1}^{+1} \gamma_o \left\{ \frac{f_{3_u}}{f_{2_u}^{\,4}} + a\,\frac{f_{3_u}(a^2+h^2) - 2\left(\frac{b_o}{2}\eta_o' - \frac{b_u}{2}\eta_u\right)^4}{f_{1_u}^{\,3}\, f_{2_u}^{\,4}} \right\} d\,\eta_o' \\
&\qquad \text{(downwash due to trailing vortex)} \\
&\left. + \frac{t_u}{4}\int_{-1}^{+1} \gamma_o \left\{ \frac{1}{f_{1_u}^{\,3}} - \frac{3\,h^2}{f_{1_u}^{\,5}} \right\} d\,\eta_o' \right] \qquad \text{(curvature effect)}
\end{aligned}\right\} \quad (5)$$

The sketches (figs. 4 and 5) serve to clarify the signs of the angles of attack induced by the interference.

It is particularly worthy of note in these equations that the parameters do not always enter linearly. The term which characterizes the change in the longitudinal velocity is square with respect to the angle of attack (in γ_o there occurs α_o as a factor). The advantages of the linear theories, for example, the possibility of obtaining the total circulation through the superposition of the simple basic distributions are thus lost.

For our computation, we have only made the assumptions which are made for the individual wings of the Prandtl airfoil theory. For the determination of the angles of attack

induced by interference, the cellule may be of arbitrary shape. The two equations lead to the following conclusions as to the mutual interference of the wings of a biplane cellule:

1. In general, the interference effect decreases with increasing stagger h;

2. At the upper wing $\alpha_{i_{ou}}$ increases with increasing span of the lower wing;

3. At the lower wing there similarly is a larger $\alpha_{i_{uo}}$ corresponding to a larger span of the upper wing;

4. If $a > 0$ (forward camber) almost all factors tend to a decrease in the effective angle of attack at the lower wing, whereas at the upper wing various effects may cancel each other. It is even possible with larger stagger to obtain an increase in the effective angle of attack for the upper wing. Forward stagger always affects the lower wing more than the upper.

5. If $a < 0$ essentially the reverse of the above holds true.

In order to obtain an idea as to the order of magnitude of the various factors each is plotted for the upper wing of a recent biplane (example III) in figure 6, where there is also included a plot of the self-induced angle of attack.*

The combined effect of all the factors results in downwash over the greatest portion of the span, so that $\alpha_{i_{ou}}$, according to equation (1), is mostly positive (in fig. 6 the positive direction is downward). The greatest effect is that shown by the tip vortices for which the part corresponding to the unstaggered cellule (term without a in (4)) is most prominent. The effect of the trailing

---

*With regard to the peaks that occur in the α_{i_o} curve, it is to be observed that these are due to a discontinuity in the twist of the upper surface.

vortices on the curvature of the streamlines is slight as was mentioned above. The curvature is mainly to be ascribed to the effect of the lifting vortex. The lifting vortex also exerts an effect through a change in the longitudinal velocity and through upwash although these effects are relatively small. From figure 6 the important fact is to be noted that in a more accurate theory all terms in equations (4) and (5) must be taken into account.*

For determining the required γ_o and γ_u, we thus have the two integrodifferential equations (4) and (5), whose particularly inconvenient property is that it is not possible to effect a separation into two equations for γ_o and γ_u.

IV. METHOD OF SOLUTION

A solution of these two equations for γ_o and γ_u in closed form is hardly worth attempting. We shall thus try to determine the circulations from equations (4) and (5) by an approximation method where we may assume that the interference and self-induced angles of attack are small compared with the others.

We first solve the equations for the monoplanes

$$\frac{\gamma_o b_o}{c_{l_o} t_o} = \alpha_o - \frac{1}{2\pi} \int_{-1}^{+1} \frac{d\gamma_o}{d\eta_o'} \frac{d\eta_o'}{\eta_o' - \eta_o}$$

and

$$\frac{\gamma_u b_u}{c_{l_u} t_u} = \alpha_u - \frac{1}{2\pi} \int_{-1}^{+1} \frac{d\gamma_u}{d\eta_u'} \frac{d\eta_u'}{\eta_u' - \eta_u}$$

---

*That the sum of all the parts in figure 6 approximately agrees with the effect of the trailing vortices is to be ascribed to the special shape of cellule III and cannot be assumed as true in general.

by the method of H. Multhopp (reference 47) and obtain from these the zero approximation $\gamma_o^{(0)}$ and $\gamma_u^{(0)}$. With these values, we next compute from equations (4) and (5), $\alpha_{i_{ou}}(\gamma_u^{(0)})$ and $\alpha_{i_{uo}}(\gamma_o^{(0)})$ (the integrations are performed graphically) and substitute these values in the equations as a twist, that is, to be added to α_o and α_u, and from these new values $\gamma_o^{(1)}$ and $\gamma_u^{(1)}$ are determined, and thus the biplane interference effects accounted for to a first approximation. Similarly we obtain $\gamma_o^{(2)}$ and $\gamma_u^{(2)}$, etc. In this manner a well converging iteration process is made possible which gives us values for γ_o and γ_u sufficiently accurate for practical purposes even after the first, but at most after the third approximation. Having determined with sufficient accuracy the values of γ, we may compute the induced angle of attack α_i, the total lift coefficients of each wing $\overline{c_a}$, the induced drag coefficient c_{wi}, the rolling moment coefficient c_{mq}, and the coefficient for the induced pitching moment c_{msi} for each wing and for the cellule in the usual manner, as well as the remaining magnitudes depending on the lift distribution (see section II).

As regards the practical carrying-out of the computation the following may be said. The integrals of equations (4) and (5) are made up of a few components that for the most part may be obtained graphically (see figs. 2 and 3). The determination of the approximations is particularly simple, since in the system of equations to be solved by the method of Multhopp, only the terms involving the twist portion vary. All the computations may be carried out by employing technical aids. The time required is about a week for simple biplane arrangements up to three weeks for more complicated arrangements. Experienced computers can still further reduce the time considerably.

V. GENERALIZATION OF THE METHOD

Up to the present we have assumed that each wing may be replaced by a lifting vortex filament. It appears, how-

ever, that this assumption is not sufficient in some particular cases. The first difficulty occurs in the determination of the stagger a. We had assumed that the center of pressure at each section of each wing lies on straight lines and denotes the distances between these two lines in the x direction by a. It is evident that in the neighborhood of the zero lift of a wing this method leads to contradictions since the center of pressure then travels off to infinity. Furthermore, very close to a wing the velocity field due to the substitution vortex does not agree sufficiently with that of a wing of finite chord, thickness, and camber. We are thus constrained to improve the theory given above for the range near the zero lift and the case of wings of small gap. A comparison of the computations and measurements given below will show, however, that the simple theory with a single vortex element is sufficiently accurate in most cases if the gap-chord ratio is equal to or greater than 1. To present the relations correctly it would be necessary to replace each wing by a lifting surface. A step in this direction is the following method, which already gives sufficiently good results.

We replace each wing by two straight-line vortices at right angles to the flow and having strengths Γ_1 and Γ_2, the position of the vortices being assumed at 1/4 and 1/2 chord, respectively, from the leading edge of the wings.* This method has the following advantages. In the first place, by using two vortices the velocity field is more accurately represented. In the next place it is now possible at each position along the span to have the center of pressure of each of the substitution vortices agree with the actual center of pressure at each wing section by suitable distribution of the circulation of the two vortex elements. If only a single lifting vortex element is assumed, it is impossible to take into account deviations of the centers of pressure from the straight lines. Finally, on the assumption of two vortex elements, it is possible, in addition to effects on the angles of attack, also to consider more accurately the curvature of the streamlines due to the interference. Since the first vortex element is assumed at 1/4 chord and the second at 1/2 chord from the leading edge, the forward element, according to the

---

*More general singularity substitutions for the two-dimensional biplane problem will be found, for example, in E. Pistolesi (reference 20).

theory, will take up the effects of the angle of attack and the rear element, those of the streamline curvature. Practically, however, these effects are not so easily separated.

We must first set up a theory of the monoplane wing which is replaced by two lifting vortices. It is to be noted, however, that this theory is of use only in regard to our final object since in the case of the monoplane alone the self-induced curvature of the streamlines is so small that it may be neglected. In addition to the angle of attack equation

$$\alpha_e = \alpha_g - \alpha_i \tag{6}$$

we have the relation

$$f_e = f_g - f_i \tag{7}$$

for the camber f denoting in general the rise in camber of the section. In these equations we must express α_e, f_e, and α_i, f_i through the circulations of the two lifting vortices. To determine α_e and f_e, we consider the relations at a wing cross section. For the lift and moment coefficient the following relations hold with good approximation

$$\left.\begin{aligned} c_a &= c_a' \left(\alpha_e + \frac{2 f_e}{t}\right) \\ c_m &= c_m' \left(\alpha_e + \frac{4 f_e}{t}\right) \end{aligned}\right\} \tag{8}$$

with

$$c_a' = \left(\frac{d\, c_a}{d\, \alpha}\right)_{\Lambda \longrightarrow \infty}$$

$$c_m' = \left(\frac{d\, c_m}{d\, \alpha}\right)_{\Lambda \longrightarrow \infty}$$

We must further express c_a and c_m in terms of the circulations Γ_1 and Γ_2 of the lifting vortex elements in

order that we may have the relation between α_e, f_e, and Γ_1, Γ_2. A relation between these magnitudes is given by the requirement that the strength of the vortices Γ_1 and Γ_2 be such that the total lift and total moment at each wing section is not changed by the double vortex substitution.*

$$\Gamma_1 + \Gamma_2 = \frac{c_a}{2} V t \tag{9}$$

$$\frac{1}{4}\Gamma_1 + \frac{1}{2}\Gamma_2 = \frac{c_m}{2} V t \tag{10}$$

With the aid of these relations and equations (8), there is obtained

$$\alpha_e = 2\frac{\Gamma_1 + \Gamma_2}{\frac{c_a'}{2} V t} - \frac{1}{2}\frac{\frac{1}{2}\Gamma_1 + \Gamma_2}{\frac{c_m'}{2} V t} \tag{11}$$

$$f_e/t = -\frac{1}{2}\frac{\Gamma_1 + \Gamma_2}{\frac{c_a'}{2} V t} + \frac{1}{4}\frac{\frac{1}{2}\Gamma_1 + \Gamma_2}{\frac{c_m'}{2} V t} \tag{12}$$

In equations (6) and (7) there are still to be determined α_i and f_i. For this we required the sum of all induced downwash velocities w at the midpoint $(x = -t/4)$ and we obtain

$$\alpha_i = w/V \quad \text{and} \quad \frac{f_i}{t} = \frac{t}{8R} = \frac{1}{8}\frac{\partial(w/V)}{\partial(x/t)}$$

---

*The horizontal components of the disturbance velocity, which produces Γ_1 at the position of Γ_2 and Γ_2 at the position of Γ_1 is assumed small in comparison with V and its effect is therefore neglected.

where R is the radius of curvature at the center of the wing section through self-induction of the curved streamline. The value of w is determined by a method of section III, which need not be gone into here. We obtain finally from equations (6) and (7) with (11) and (12), setting $\gamma = \Gamma / b V$:

$$2 \frac{\gamma_1 + \gamma_2}{\frac{c_a' t}{2 b}} - \frac{1}{4} \frac{\gamma_1 + 2 \gamma_2}{\frac{c_m' t}{2 b}} =$$

$$= \alpha_g - \frac{1}{2 \pi} \int_{-1}^{+1} \frac{d \gamma_1}{d \eta'} \left[1 + \frac{2 b}{t} \sqrt{\left(\frac{t}{2 b}\right)^2 + (\eta - \eta')^2} \right] \frac{d \eta'}{\eta - \eta'} -$$

$$- \frac{1}{2 \pi} \int_{-1}^{+1} \frac{d \gamma_2}{d \eta'} \frac{d \eta'}{\eta - \eta'} \qquad (13)$$

$$- \frac{\gamma_1 + \gamma_2}{\frac{c_a' t}{2 b}} + \frac{1}{4} \frac{\gamma_1 + 2 \gamma_2}{\frac{c_m' t}{2 b}} =$$

$$= \frac{2 f_g}{t} - \frac{b}{\pi t} \int_{-1}^{+1} \frac{d \gamma_1}{d \eta} \frac{\eta - \eta'}{\sqrt{\left(\frac{t}{2 b}\right)^2 + (\eta - \eta')^2}} d \eta' +$$

$$+ \frac{t}{4 \pi b} \int_{-1}^{+1} \frac{d \gamma_2}{d \eta'} \frac{\eta - \eta'}{\sqrt{\left(\frac{t}{2 b}\right)^2 + (\eta - \eta')^2}} d \eta' \qquad (14)$$

There are thus set up the monoplane equations based upon the assumption of two vortex elements for each wing. These equations may be solved by iteration by determining, for example, as a rough approximation the sum $\gamma_1 + \gamma_2$

according to the usual airfoil theory, separating into γ_1 and γ_2 according to the two-dimensional theory (equations (9) and (10)) and then using these as initial values for the iteration process, substituting in the right sides of equations (13) and (14).

Through the biplane interference effects, the longitudinal velocity, the angle of attack, and the curvature of the flow are changed by amounts ΔV_2, $\Delta \alpha_2$, Δf_2, and from these there is obtained a change in Γ_1 and Γ_2 by amounts $\Delta\Gamma_1$ and $\Delta\Gamma_2$ given by*

$$\Delta\Gamma_1 = \Gamma_1 \frac{\Delta V_2}{V} + \frac{\partial \Gamma_1}{\partial \alpha} \Delta \alpha_2 + \left[\frac{\partial \Gamma_1}{\partial f} \Delta f_2 \right]$$

$$\Delta\Gamma_2 = \Gamma_2 \frac{\Delta V_2}{V} + \left[\frac{\partial \Gamma_2}{\partial \alpha} \Delta\alpha_2 \right] + \frac{\partial \Gamma_2}{\partial f} \Delta f_2$$

These equations may also be put in the form**

$$\left.\begin{aligned} \Delta\gamma_1 &= \gamma_1 \frac{\Delta V_2}{V} + c_{a_1}' \frac{t}{2b} \Delta\alpha_2 + \left[\frac{c_{a_1}' \Delta f_2}{b} \right] \\ \Delta\gamma_2 &= \gamma_2 \frac{\Delta V_2}{V} + \left[c_{a_2}' \frac{t}{2b} \Delta\alpha_2 \right] + \frac{c_{a_2}' \Delta f_2}{b} \end{aligned}\right\} \quad (15)$$

In these equations we determine c_{a_1}' and c_{a_2}' by plotting first $c_a(\alpha_\infty)$ for the entire wing and separating in-

---

*Since according to the theory $c_m' = c_a'/4$ the terms in the square brackets drop out because $\frac{\partial \Gamma_1}{\partial f} = 0$ and $\frac{\partial \Gamma_2}{\partial \alpha} = 0$. Actually this assumption holds generally only within a restricted range of angle of attack. It is necessary to carry these terms along in some cases, therefore.

**It is here assumed as above that the familiar relation $c_a = c_a'(\alpha_e + 2 f_e/t)$ holds for each wing, see formula (8).

to c_{a_1} and c_{a_2} according to equations (9) and (10). The slopes of these curves give us the required values. It will then appear whether or not $c_{a_2}' = 0$, i.e., whether or not the separation was necessary. If we now substitute in these equations for the disturbance values, the expressions obtained in section III and also in equations (13) and (14) $\gamma_1 + \Delta\gamma_1$ and $\gamma_2 + \Delta\gamma_2$ in place of γ_1 and γ_2, respectively, we have the new integrodifferential equations, which must be satisfied by γ_1 and γ_2. There are obtained altogether four equations for the four unknowns γ_{o_1}, γ_{o_2}, γ_{u_1}, and γ_{u_2}.

VI. RESULTS OF THE COMPUTATION

We shall now make use of the above method to compute the lift distributions of several types of airplanes. Of the five models computed (fig. 7), measurements on only the first three were available for comparison. Models IV and V were freely chosen, the former representing the conventional biplane cellule (two equal rectangular wings with rounded-off corners of aspect ratio 6 and gap-chord ratio 1). The computation was performed for zero and moderate forward stagger of the upper wing. Model V represented the limiting case of the sesquiplane with elliptical wings. In presenting the results, there was first computed the total lift coefficient $\overline{c_a}$ from the formula

$$\overline{c_a} = \Lambda \int_{-1}^{+1} \gamma \, d\eta$$

for each wing and for the biplane arrangement and the values plotted against α. The angles of attack induced by the mutual interference and the spanwise lift distributions are given in section VII below where a comparison is made of the various models. Unfortunately, only in the case of model I was it possible to compare the lift distributions with the results of measurements.

Example 1: The computation was first carried out for the cellule of a rather old type airplane* (model I), the

*Shape of cellule and other data as in the case of the remaining examples are given in figure 7.

American single-seat pursuit airplane PW-9 for which detailed measurements were available (references 38 and 39). This example was chosen because pressure distribution measurements on each wing and on the biplane arrangement were available so that the computation could be compared with the results of tests. In figures 8 and 9 the computed and measured distribution of $\gamma = c_a \, t/2 \, b$ was plotted against the span for each wing for various angles of attack. It is seen that there is good agreement between the two. On the upper wing the first approximation is already sufficiently accurate while for the lower wing, for which the deviation from the undisturbed wing is considerably greater, a second approximation was necessary. A third approximation would only slightly affect the results. The total lift $\overline{c_a}$ is plotted for each wing as a function of the angle of attack in figures 10 and 11. The indicated test results of Fairbanks and Loeser (differing somewhat from each other) show that the computation lies entirely within the range of measuring accuracy.

Example 2: Model II (fig. 7) is a biplane cellule dating from the Gottingen measurements at the time of the World War (reference 28). We were led to measurements on this model as a result of a still unpublished work by R. Fuchs, where for this particular example no satisfactory agreement in the $\overline{c_a}$ values between the computation and measurements could be attained. This model has the peculiar property of having the lower wing set at 4° less than the upper wing. Moreover the gap-chord ratio is quite small ($h/t = 2/3$). With regard to the measured values there is to be observed the following. In the case of the old Gottingen measurements, the stagger could not accurately be held at the constant value 0.5 t on which the computation of Fuchs and also our own computation was based. Thus the measured values for the lower wing are derived from the value $a = 0.5$ t and those of the upper wing from the value $a = 0.547$ t. These measurements were then recomputed in terms of $a = 0.5$ t (in fig. 12 both values are plotted) so that some uncertainty is attached to the points indicated.

In carrying out the computation, it appeared that the method involving a single lifting vortex filament for each wing was not adequate, the main reason for which was to be found in the small gap of the biplane. In addition, a refinement in the computation was necessary for the cellule angle-of-attack range in the neighborhood of zero degrees.

In this range the lower wing has practically no lift while the measurements on the upper wing, which was still 4° removed from the zero lift angle showed an effect by the presence of the lower wing (figs. 12 and 13). We therefore made use of the method given in section V above. We first replaced the lower wing in the angle-of-attack range in question by two lifting vortex elements while still using a single vortex element for the upper wing. The result was that also at the upper wing at $\alpha = 0^\circ$ there was an increase in lift and at the lower wing a decrease in lift as compared with the values obtained on the assumption of a single vortex for each wing. The agreement with the measured values was still not quite sufficient. We therefore attempted to improve the computation by the assumption of two lifting vortex filaments for each wing. This gave an increase in lift for the upper wing over the entire angle-of-attack range, so that good agreement was obtained with the measurements. Sufficiently good agreement was in this manner obtained also for the lower wing.

Example 3: The cellule of a modern type airplane* (fig. 7, model III) served as the next example. Figures 14 and 15 again show the measured and computed decrease in the total lift coefficient for the upper and lower wing and it is seen that the computation sufficiently accurately represents the conditions. The deviation from the undisturbed wing is in this case not as large as in the previous examples. A more exact comparison of the three cases will be given below (section VII). In the neighborhood of zero angle of attack of the wing, the method given in section V was used, each wing being replaced by two lifting lines. For this example we also computed the lift distribution for each wing for several deflections of the ailerons, which were located on the upper wing. Figure 16 shows the externally induced angle of attack $\alpha_{i_{uo}}$ at the lower wing for an aileron deflection $\beta_{Q_o} = \pm 1$ ($\beta_{Q_o} = +1$ on the right wing and -1 on the left). The lift distribution of the upper wing is shown in figure 17 and that of the lower wing in figure 18 for various aileron deflections ang angles of attack. The effective rolling-moment coefficient c_{m_q} for the entire cellule would be, without interference, $+0.582$ for $\beta_{Q_o} = \pm 10^\circ$ and $+1.166$ for $\beta_{Q_o} = \pm 20^\circ$. On account of the modified lift distribution of the lower wing, an effective rolling moment in the opposite direction is produced so that the total rolling-moment coeffi-

*The test results were kindly made available to us by the manufacturers.

cient of the biplane cellule is only +0.564 for $\beta_{Q_o} = \pm 10^o$ and +1.13 for $\beta_{Q_o} = \pm 20^o$. (The angle of attack enters practically linearly and therefore has only a slight effect on c_{m_q}.) Measurements of this kind that could be used for comparison were not available. The relations given are naturally valid for conditions below the flow separation point. The effect of the change in the lift distribution as compared with that of the monoplane on the separation will be discussed later (section VII).

Example 4: The computation for model IV (fig. 7) was carried out once for the unstaggered biplane (a = 0; IVa) and again for the staggered biplane (a/h = +0.45; IVb) by the method of section IV. Since the upper and lower wings are equal, the computation was very simple as many expressions could be determined with the two wings in common. Figures 19 and 20 show the total lift coefficients as a function of the angle of attack for each wing and bring out the effect of stagger. The result showed that the upper wing of the staggered cellule experiences hardly any decrease in lift as compared with the unaffected wing, while the decrease is stronger for the lower wing, so that as a whole the cellule experiences a decrease in lift. Figures 19 and 20 further show that the third approximation is also sufficient for this case where the mutual interference is relatively large. In figure 21 are shown the polars* for the upper wing, lower wing, and cellule, which, in case of equal wings must approximately agree. This is at the same time a check on the accuracy of the measurements and shows that in spite of the many graphical integrations the computation was carried out with sufficient accuracy.

Example 5: To complete the series of examples, there was computed as a final example a cellule for which the span of the lower wing was half as large as that of the upper wing, i.e., a sesquiplane (model V, fig. 7). The wings of the freely chosen cellule are elliptical. Further, the gap between the wings was chosen relatively small ($h/t_o = 0.75$). In the rather large resulting interference effect, which changed the elliptic lift distribution considerably, it was necessary to carry out the computation for each wing as far as the third approximation. Figures 22 and 23 show, however, that a further refinement is not necessary.

---

*$\overline{c_{w_i}}$ was determined from the lift distributions from $\overline{c_{w_i}} = \Lambda \int_{-1}^{+1} (\alpha_i \gamma)\, d\eta$.

VII. COMPARISON OF THE VARIOUS EXAMPLES

We shall now compare the results for the various models with regard to several aerodynamical characteristics. For this purpose there was plotted on figure 24 the interference angle of attack at the upper and lower wing of each model for the angle of attack 5° (above zero angle of attack) of the cellule so that the mutual interference effects could be compared in each case. Further, in figures 25 to 29 are plotted the ratio $\frac{c_a\, t}{\overline{c_a}}$, the chord t, and the ratio of the local c_a values to the total $\overline{c_a}$ value of the wing under consideration. Figures 25 to 29 therefore give us information as to the position along the span at which there is overload and underload, respectively, and thus show where the flow will first separate in the neighborhood of $\overline{c_a}_{max}$. From the standpoint of rolling stability, it is desirable that the middle portions of the spans have a larger local c_a than the outside portions, since in that case the separation will start in the neighborhood of the fuselage and spread out toward the wing tips. Otherwise, separation starts at the wing tips, a result which may easily lead to loss in lateral stability. It is readily seen that an upwash induced at the wing tips due to interference opposes a favorable lift distribution without interference effect. The effect will be unfavorable in the neighborhood of $\overline{c_a}_{max}$ particularly with regard to the effectiveness of the ailerons which in general operate in this range. Such an upwash region is found in the case of the upper wing of model I, figure 24. The corresponding range of overload in figure 25 is shifted by the presence of the lower wing farther toward the wing tip. Since also the lower wing of this model shows the same effect to a small extent, it is to be supposed that the entire cellule will have at large angles of attack unfavorable characteristics with regard to the lateral stability.

Since the upwash region discussed above is to be ascribed to the effect of the trailing vortices, model II (fig. 26) and model IV, on account of $b_o = b_u$, cannot show this effect (fig. 24). The upwash at the upper wing of model II is due to the lifting vortex. The lower wing, however, receives a downwash of such magnitude that in

order to attain again the lift that it would have in the undisturbed flow, it would have to be set over a large part of the span at an angle 5° to 6° higher. Model II, however, does not show the unfavorable lateral stability characteristics of model I, a fact that is to be ascribed to the rectangular shapes and the equal spans of the two wings.

The most favorable characteristics in every respect are shown by model III. The mutual interference as compared with that of the other models is smallest (fig. 24). In spite of the fact that the lower wing of model III as well as that of model I has a smaller span than the upper wing ($b_u/b_o = 0.763$ for model III and 0.708 for model I), the upwash at the tips of the upper wing of model III has to some extent been avoided by suitably shaping the wings so that the good load relations (fig. 27) are not unfavorably changed to any large extent and it may be stated that this model shows good characteristics with regard to lateral stability.

With regard to model IV (fig. 28), it is worth noting that the overloading due to the interference effect is somewhat equalized as appears particularly in the lower wing of the staggered cellule IVb where $c_a t/\overline{c_a}$ and t almost agree. The upper wing of model IVb shows almost no effect (fig. 24). Otherwise, model IV shows characteristics similar to model II. The downwash at the upper wing of model IV, however, due to the larger gap h of the wings (fig. 7) is not so large (3° to 4° over a large part of the span).

The particular reason for carrying out the computation on model V was that a larger upwash region was expected at the upper wing. This expectation was confirmed by the computation (fig. 24). The effect, however, is not so large as not to be avoidable by a correspondingly moderately large twist. There is to be sure such a large change in the elliptic lift distribution (fig. 29) that the separation begins at the wing tips so that this model does not appear to have safe lateral stability characteristics. For biplane arrangements such as those of these examples, it may be said that at least for the upper wing the rectangular plan form has advantages as compared with others.

It may be pointed out in concluding that in addition to the lift distribution, it is also possible to compute the induced drag as has been done for one case (fig. 21).

A comparison with measurements gives the noteworthy result that (for example, for model III) the profile drag $\overline{c_w} - \overline{c_{w_i}}$ (where $\overline{c_w}$ is taken from measurements) was quite considerably increased at the lower wing through the effect of the upper wing and showed a dependence on the angle of attack (fig. 30). To explain this it would be necessary to investigate the pressure and velocity relations in the boundary layer of the lower wing, which, however, would lead us beyond the confines of this report.

VIII. SUMMARY

After a brief review of the work that has so far been done on the biplane problem, there are set up the general equations for the circulation distribution along the span of the wings of a biplane cellule and a method of solution indicated. The assumption is first made that each wing may be replaced by a vortex element in the sense of the Prandtl airfoil theory. In the examples computed it appeared that this assumption was sufficient for the usual biplane arrangements and the results of the computation show good agreement with the measurements. A refinement of the theory is necessary, however, in the neighborhood of zero angle of attack and for the case of very small gap-chord ratio. By the assumption of a double vortex system at each wing, better agreement is obtained and the curvature of the streamlines is likewise better taken into account. With this assumption, there is first set up a theory of the monoplane and this theory is then applied to the biplane. With the aid of five examples, which cover the range of usual biplane arrangements, it is shown how large is the additional angle of attack induced at each wing by the presence of the other. The examples are also compared with regard to stability about the longitudinal axis in the neighborhood of $\overline{c_a}_{max}$.

The author is very grateful for the many valuable suggestions of Miss I. Lotz during the conduct of this investigation.

Translation by S. Reiss,
National Advisory Committee
for Aeronautics.

REFERENCES

1. Betz, A.: Die gegenseitige Beeinflussung zweier Tragflächen. Z.F.M., Bd. 5, Heft. 18 and 19, Oct. 17, 1914, S. 253-58.

2. Betz, A.: Berechnung der Luftkräfte auf eine Doppeldeckerzelle aus den entsprechenden Werten für Eindeckertragflächen. T.B., Bd. 1, Heft. 4, June 1, 1917, S. 103.

3. Prandtl, L.: Der induzierte Widerstand von Mehrdeckern. T.B., Bd. 7, Heft. 7, S. 309.

4. Prandtl, L., and Betz, A.: Vier Abhandlungen zur Hydrodynamik und Aerodynamik. Göttingen 1927. Tragflügeltheorie II. Mitteilung.

5. Von Sanden, H.: Interference of Multiplane Wings Having Elliptical Lift Distribution. T.N. No. 181, N.A.C.A., 1924.

6. Bose, N. K., and Prandtl, L.: Beiträge zur Aerodynamik des Doppeldeckers. Z.a.M.M., Bd. 7 (1927), S. 1-9. Vgl. auch die vollständige Dissertation (Göttingen 1923) von N. K. Bose.

7. Fuchs, R., Hopf, L., and Seewald, F.: Aerodynamik, Bd. II. Berlin, 1934.

8. Munk, M. M.: Isoperimetrische Aufgaben aus der Theorie des Fluges. Diss. Göttingen 1919.

9. Kutta, W. M.: Über ebene Zirkulationsströmungen nebst flugtechnischen Anwendungen. Sitzungsberichte der Kgl. Bayer. Akad. der Wissenschaften. Math.-physik. Kl., München, 1911.

10. Grammel, R.: Die hydrodynamischen Grundlagen des Fluges. Friedr. Wieweg & Sohn, Braunschweig. 1917.

11. Pohlhausen, E.: Ebene Potentialströmung um Doppeldecker. Diss. Göttingen, 1919. (Auszig im Jahrbuch der Philosophischen Fakultät in Göttingen, 1921.)

12. Munk, Max M.: General Biplane Theory. T.R. No. 151, N.A.C.A., 1922.

13. Eck, Bruno: Neuartige Berechnung der aerodynamischen, Eigenschaften eines Doppeldeckers. Z.F.M., Bd. 16, Heft 9, May 14, 1925, S. 183-94.

14. Moriya, T.: On the Lift of Biplanes. Jour. of the Faculty of Engineering, Tokyo Imp. Univ., vol. 17, no. 10, Aug. 1928, pp. 191-200.

15. Glauert, H.: Tragflügel und Luftschraubentheorie. Übersetzung von Holl., Berlin, 1929.

16. Lagally, M.: The Frictionless Flow in the Region Around Two Circles. T.M. No. 626, N.A.C.A., 1931.

17. Millikan, Clark B.: An Extended Theory of Thin Airfoils and Its Application to the Biplane Problem. T.R. No. 362, N.A.C.A., 1930.

18. Tani, I.: On the Approximate Calculation of the Lift of a Biplane. Jour. of the Society of Mechanical Engineers, Japan. (Foreign edition) vol. 34, no. 6, 1931, pp. 33-37.

19. Ferrari, C.: Sul problema del biplano di apertura finita. L'Aerotecnica, vol. 13, nos. 1-2, Jan.-Feb. 1933, pp. 39-57.

20. Pistolesi, E.: Considerazioni sul problema del biplano. L'Aerotecnica, vol. 13, no. 3, Mar. 1933, pp. 185-93.

21. Schmitz, G.: Beitrag zur Theorie der ebenen wirbelfreien Strömung um den Doppeldecker. Ann. d. Phys. 5, Folge Bd. 21, 1934, S. 37.

22. Teofilato, P.: Contributo allo studio del biplano indefinito e al problema della minima resistenza per il biplano finito. Acta Pontif. Acad. Sci. Novi Lyncaei, vol. 87, 1934, p. 447.

23. Bonder, J.: Konforme Abbildung des Äusseren zweier beliebiger Kreisbogen auf das Äussere zweier Kreise. Warszawa, Wydane z Zapomogi Akad. Nauk Techn., 1935.

24. Koebe, P.: Hydrodynamische Potentialströmungen in mehrfach zusammenhängenden ebenen Bereichen im Zusammenhang mit der konformen Abbildung solcher Bereiche. Bericht der Math.-Physik. Klasse der sächsischen Akad. d. Wissenschaften, Bd. 87, 1935.

25. Garrick, I. E.: Potential Flow about Arbitrary Biplane Wing Sections. T.R. No. 542, N.A.C.A., 1936.

26. Graeser, E.: Anwendung der Funktionentheorie auf die Theorie der Profilströmungen und damit zusammenhängende Probleme der konformen Abbildung. Deutsche Mathematik, Bd. 1, 1936, S. 825.

27. Nénadovitch, M.: Recherches sur les cellules biplanes rigides d'envergure infini. Publications sci. et techn. du ministère de l'air, No. 86, 1936.

28. Munk, Max M.: Beitrag zur Aerodynamik der Flugzeugtragorgane. T.B., Bd. 2, Heft 2, March 20, 1918, S. 187.

29. Cowley, W. L., and Levy, H.: The Contribution of the Separate Planes to the Forces on a Biplane (R.A.F. 15 Section). R. & M. No. 589, British A.C.A., 1919.

30. Cowley, W. L., and Lock, C. N. H.: Biplane Investigation with R.A.F. 15 Section. R. & M. No. 774, British A.R.C., 1921.

31. Cowley, W. L., and Jones, L. J.: Biplane Investigation with R.A.F. 15 Section. Part II. R. & M. No. 857, British A.R.C., 1922.

32. Ergebnisse der Aerodynamischen Versuchsanstalt zu Göttingen. II. Lieferung. München, 1923.

33. Norton, F. H.: Pressure Distribution over the Wings of an MB-3 Airplane in Flight. T.R. No. 193, N.A.C.A., 1924.

34. Parkin, J. H., Shortt, J. E. B., and Heard, C. G.: Pressure Distribution over U.S.A. 27 Aerofoil with Square Wing Tips. Aeron. Res. Paper, No. 18. Univ. of Toronto Bulletin No. 7, 1927, pp. 85-135.

35. Parkin, J. H., Shortt, J. E. B., and Cade, J. G.: Pressure Distribution over Göttingen 387 Aerofoil with Square Wing Tips. Aeron. Res. Paper, No. 18a. Univ. of Toronto Bulletin No. 7, 1927, pp. 137-89.

36. Parkin, J. H., Shortt, J. E. B., and Cade, J. G.: Biplane Investigation. Aeron. Res. Paper, No. 19. Univ. of Toronto Bulletin No. 7, 1927, pp. 181-221.

37. Munk, Max M.: The Air Forces on a Systematic Series of Biplane and Triplane Cellule Models. T.R. No. 256, N.A.C.A., 1927.

38. Fairbanks, A. J.: Pressure Distribution Tests on PW-9 Wing Models Showing Effects of Biplane Interference. T.R. No. 271, N.A.C.A., 1927.

39. Loeser, Jr., Oscar E.: Pressure Distribution Tests on PW-9 Wing Models from 18° through 90° Angle of Attack. T.R. No. 296, N.A.C.A., 1929.

40. Knight, M., and Noyes, R.: Wind Tunnel Pressure Distribution Tests on a Series of Biplane Wing Models. T.N.'s Nos. 310, 325, and 330, N.A.C.A., 1929.

41. Noyes, Richard W.: Pressure Distribution Tests on a Series of Clark Y Biplane Cellules with Special Reference to Stability. T.R. No. 417, N.A.C.A., 1932.

42. Pearson, H. A.: Pressure Distribution Measurements on an O-2H Airplane in Flight. T.R. No. 590, N.A.C.A., 1937.

43. Kuhn, Paul: Working Charts for the Determination of the Lift Distribution between Biplane Wings. T.R. 445, N.A.C.A., 1932.

44. Diehl, Walter S.: Relative Loading on Biplane Wings. T.R. No. 458, N.A.C.A., 1933.

45. Diehl, Walter S.: Relative Loading on Biplane Wings of Unequal Chords. T.R. No. 501, N.A.C.A., 1934.

46. Pistolesi, E.: Sul Problema dell'ala Rotante. Atti Accad. naz. Lincei, vol. 6, 1936, p. 23.

47. Multhopp, H.: Ein einfacher Weg zur Berechnung der Auftriebsverteilung von Tragflügeln. Luftfahrtforschung, Bd. 15, Heft. 4, April 6, 1938, S. 153-69.

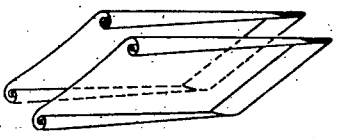

Figure 1.- The vortex system used as a basis in the investigation.

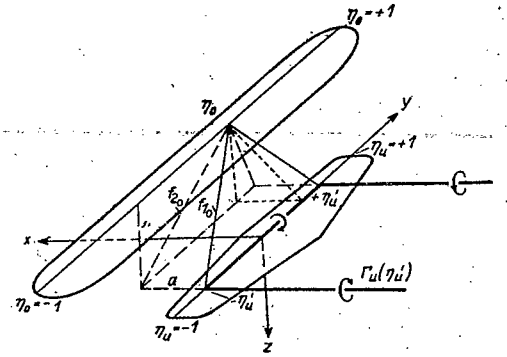

Figure 2.- Sketch for obtaining the relations at the upper wing.

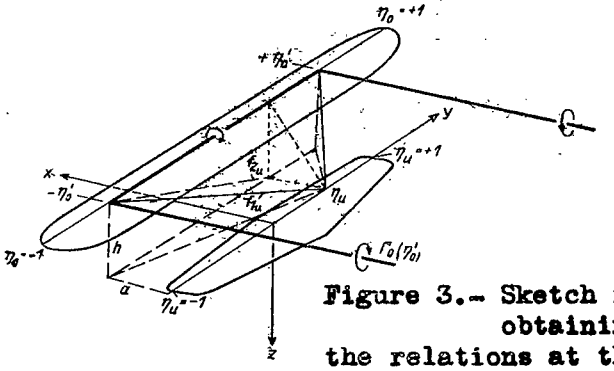

Figure 3.- Sketch for obtaining the relations at the lower wing.

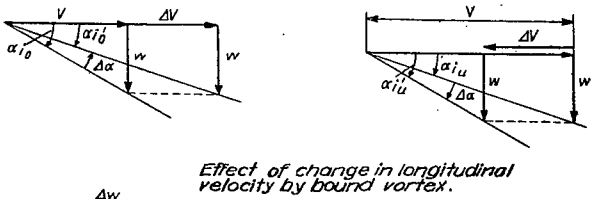

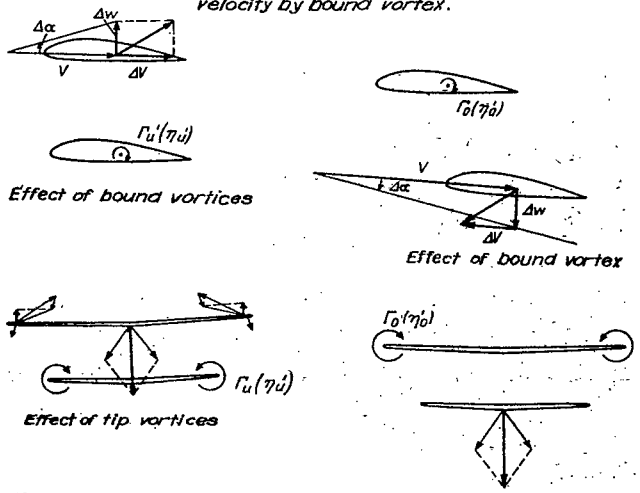

Figure 4.- Sketch showing various conditions at upper wing.

Figure 5.- Sketch showing various conditions at lower wing.

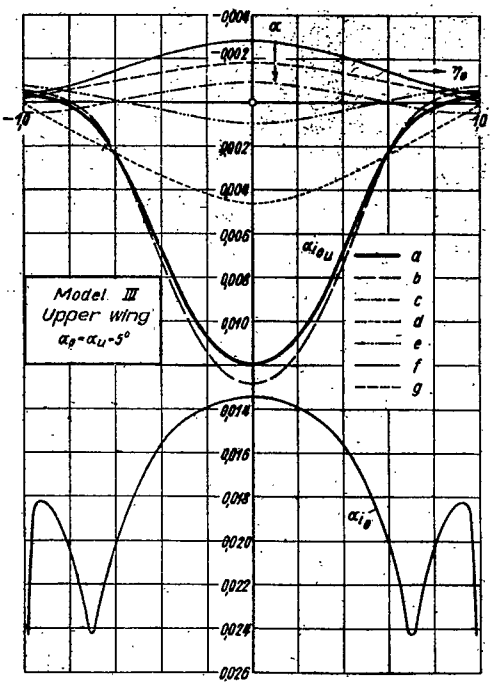

a- Total angle of attack induced by the mutual interference effect.
b- Part due to tip vortices without stagger.
c- Part due to the stagger of the tip vortices.
d- Part due to the curvature produced by the lifting vortices.
e- Part due to the curvature by the trailing vortices.
f- Part due to the lifting vortices (vertical component).
g- Part corresponding to the change in the longitudinal velocity.
Below: self induced angle of attack for comparison.

Figure 6.- Distribution of α_{iou} for model III.

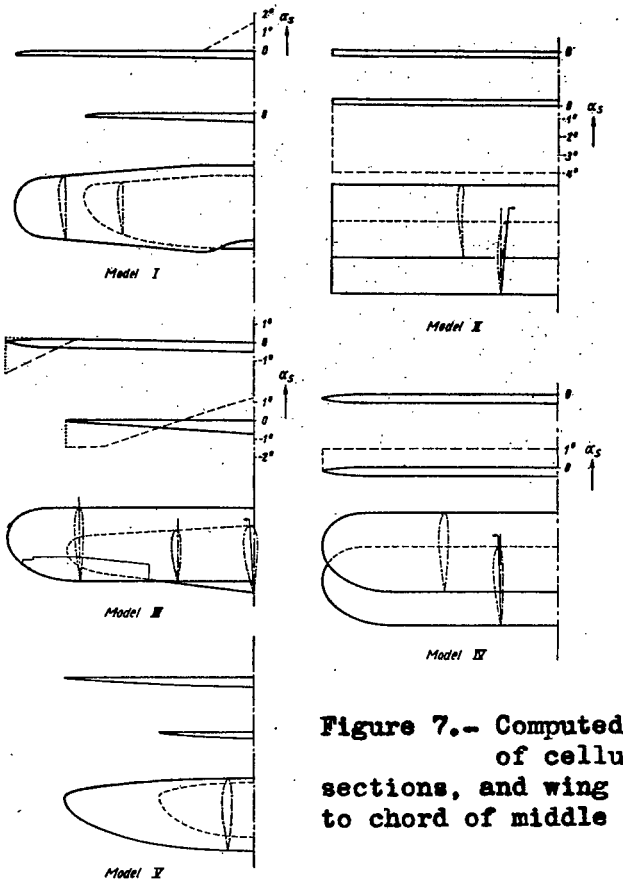

Figure 7.- Computed examples. Shapes of cellules, profile sections, and wing setting referred to chord of middle section in upper wing.

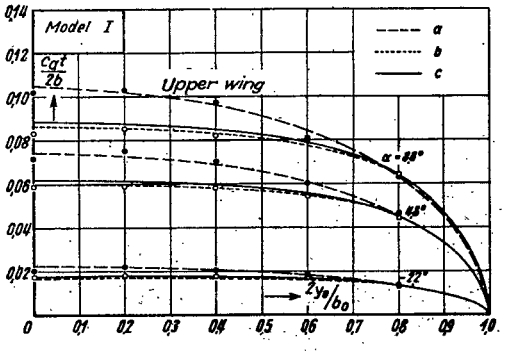

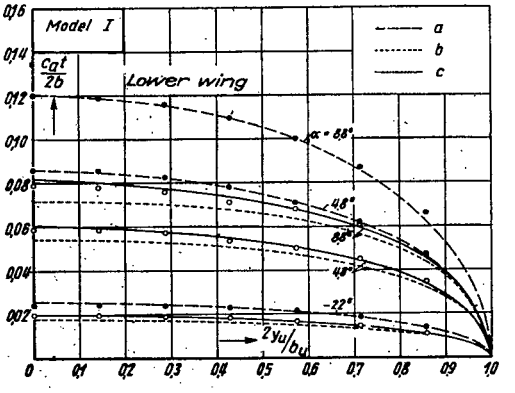

a- Wing without interference. b- Wing with mutual interference effect, first approximation. c-Wing with interference, second approximation. ●-Wing without interference measurements results. ○ - Wing with interference effect, measurement results.

Figure 8.- Distribution of circulation over the half span.

Figure 9.- Circulation distribution over the half-span.

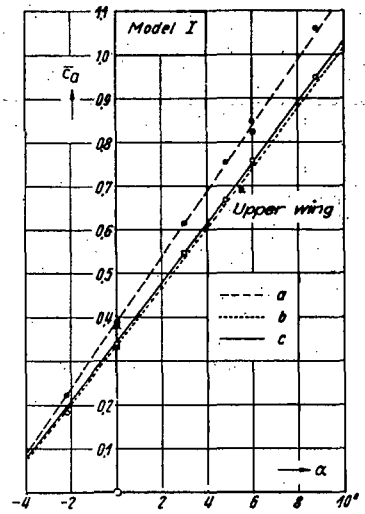

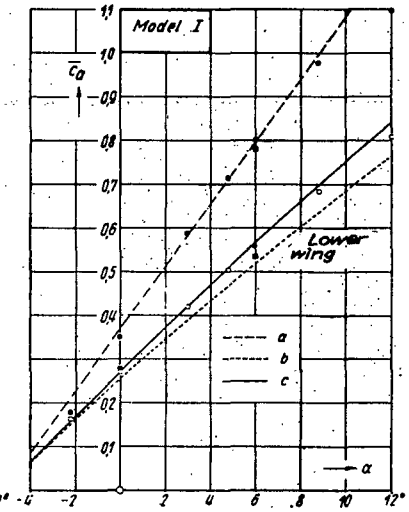

a- Wing without mutual interference. b- Wing with interference, first approximation. c- Wing with interference, second approximation. ● Wing without interference, measurements of Fairbanks. × Wing without interference, measurements of Loeser. ○ Wing with interference, measurements of Fairbanks. ⊠ Wing with interference, measurements of Loeser.

Figure 10.-Lift curves. Figure 11.-Lift curves.

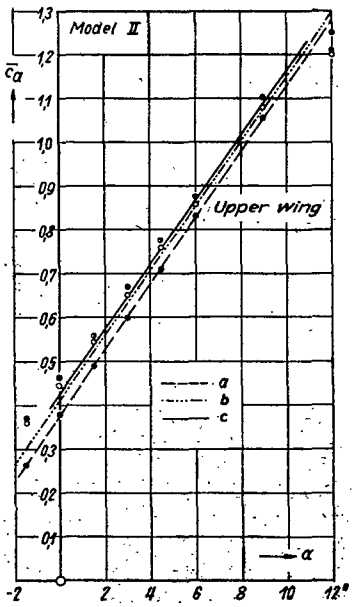

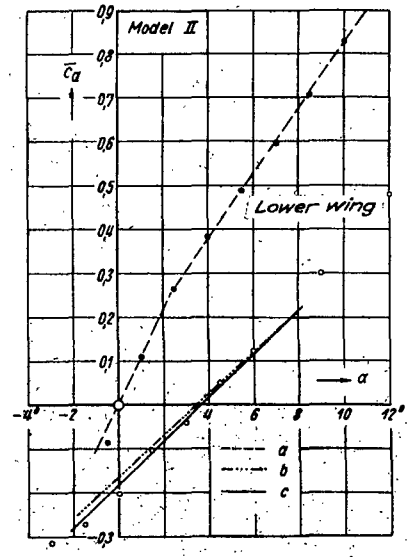

a- Wing without interference, computed. b- Wing with interference, computation with one vortex at upper wing, two in lower. c- Wing with interference, computation with two vortices in each wing. ● Wing without interference, measurement. ◑ Wing with interference, uncorrected measurement (a = 0.547 t). ○ Wing with interference, corrected measurement (a = 0.5 t).

Figure 12.- Lift curves.

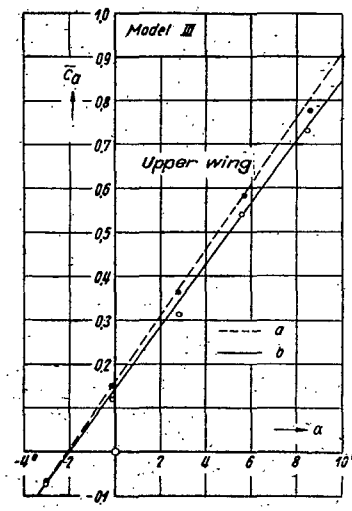

a- Wing without interference. b- Wing with interference. ● Wing without interference, measurement. ○ Wing with interference, measurement.

Figure 13.- Lift curves. (The break in curve a is only slightly noticeable in curves b and c).

Figure 14.- Lift curves.

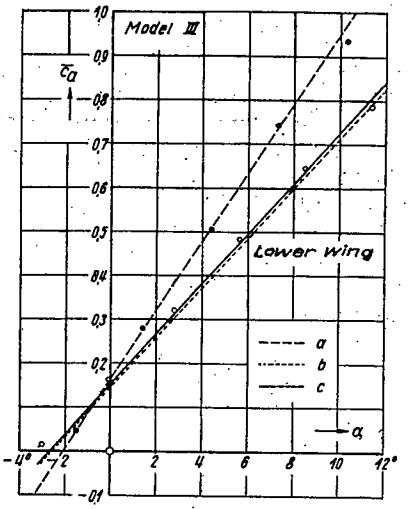

a- Wing without interference. b- Wing with interference. c- Wing with interference, second approximation. ● Wing without interference, measurement. ○ Wing with interference, measurement.

Figure 15.- Lift curves.

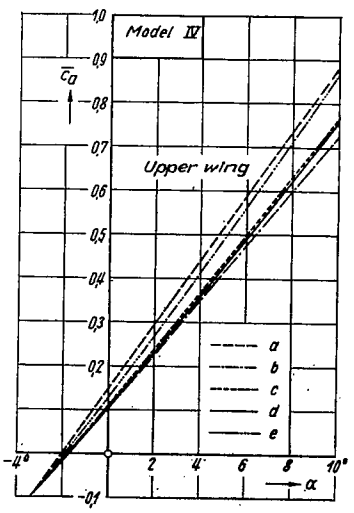

a- Wing without interference; b- wing with interference, unstaggered, first approximation; c- wing with interference, unstaggered, second approximation; d- wing with interference, unstaggered, third approximation; e- wing with interference, staggered.

Figure 19.- Lift curves.

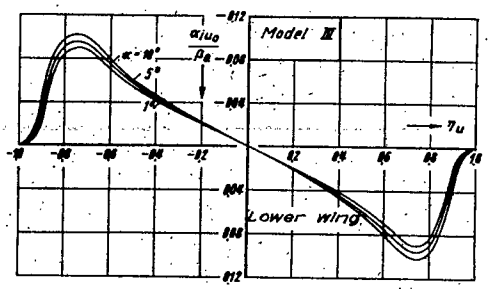

Figure 16.- Magnitude of interference angle of attack at lower wing for deflection of aileron $\beta_Q = 1$, for various angles of attack of cellule.

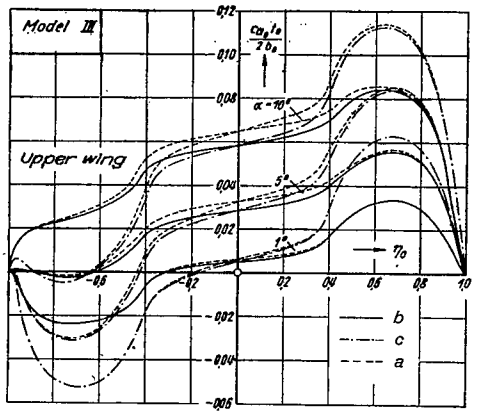

a- Without interference by the lower wing for $\beta_{Q_0} = 10°$ and 20°. b- with interference by lower wing, $\beta_{Q_0} = 10°$. c- with interference by lower wing, $\beta_{Q_0} = 20°$.

Figure 17.- Circulation distribution for aileron deflections at upper wing for various angles of attack.

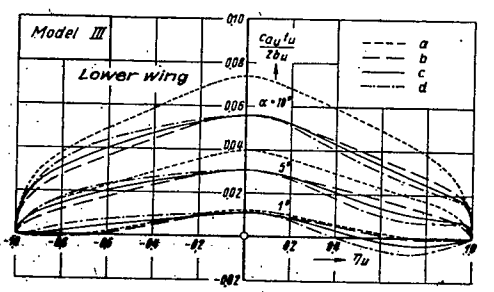

a- Without interference; b- with interference, $\beta_{Q_0} = 0°$; c- with interference, $\beta_{Q_0} = 10°$; d- with interference, $\beta_{Q_0} = 20°$.

Figure 18.- Circulation distribution for the lower wing for deflection of ailerons at upper wing.

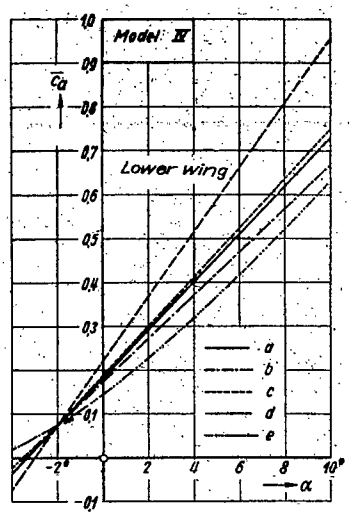

a- Wing without interference; b- wing with interference, unstaggered, first approximation; c- wing with interference, unstaggered, second approximation; d- wing with interference, unstaggered, third approximation; e- wing with interference, staggered.

Figure 20.- Lift curves.

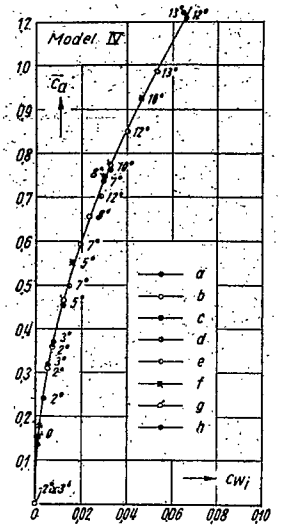

a- Upper and lower wing without interference; b- upper wing with interference, unstaggered. c- upper wing with interference, staggered; d- lower wing with interference, unstaggered; e- lower wing with interference, staggered; f- cellule wings alone; g- cellule unstaggered; h- cellule staggered.

Figure 21.- Polar diagram.

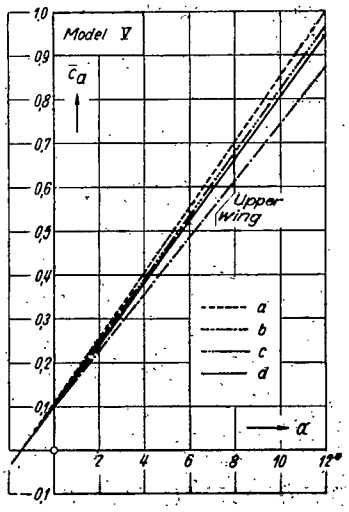

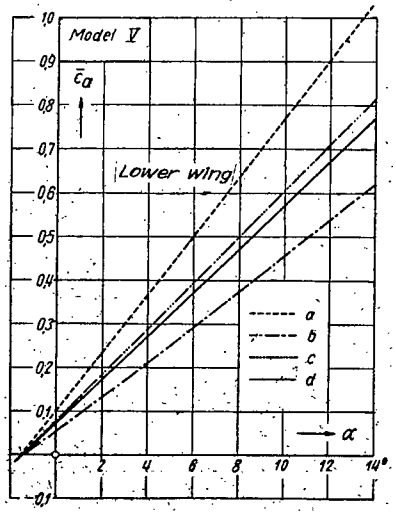

a- wings without interference; b- wings with interference, first approximation; c- wings with interference, second approximation; d- wings with interference, third approximation.

Figure 22.- Lift curves.

Figure 23.- Lift curves.

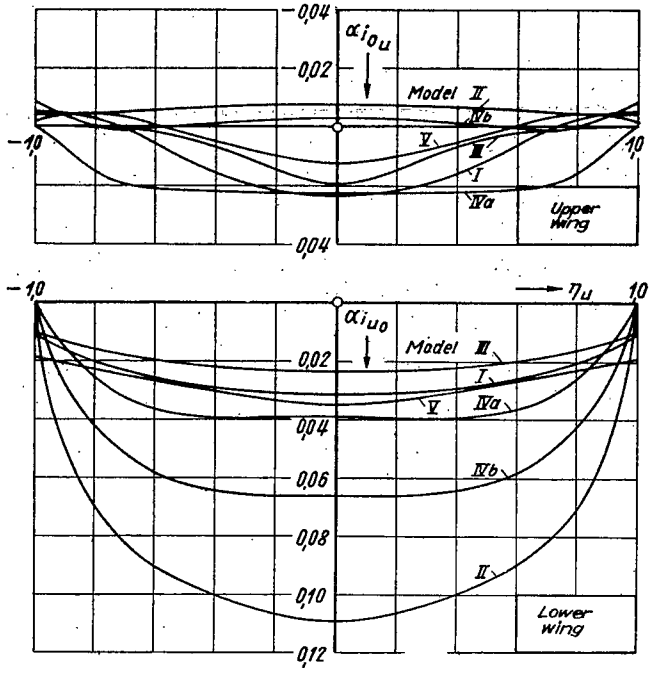

Figure 24.- Comparison of angle of attack induced by biplane interference at both wings ($\alpha = 5^\circ$ from zero angle of attack).

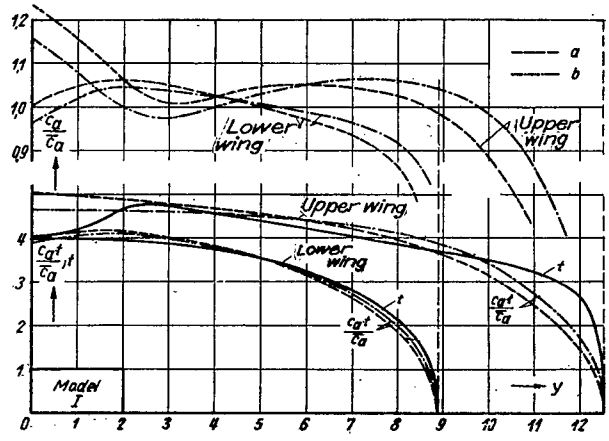

a- wings without interference;
b- wings with interference.

Figure 25.- Lift distributions.

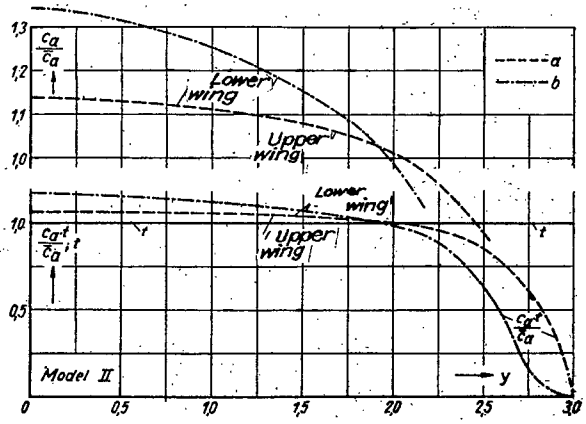

a- wings without interference;
b- wings with interference.

Figure 26.- Lift distributions. The single curve for the upper wing holds for the wing with, as well as without interference.

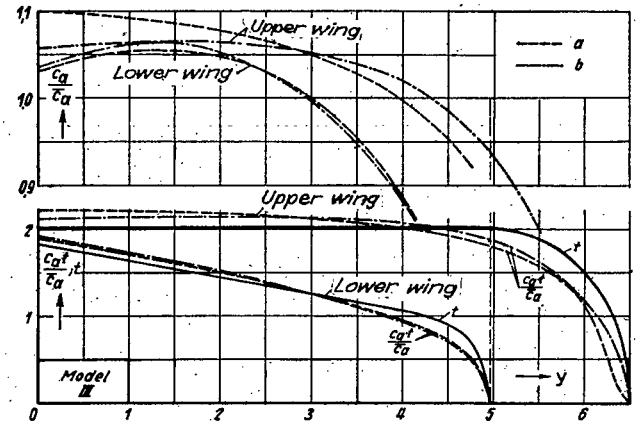

a- wings without interference;
b- wings with interference.

Figure 27.- Lift distributions.

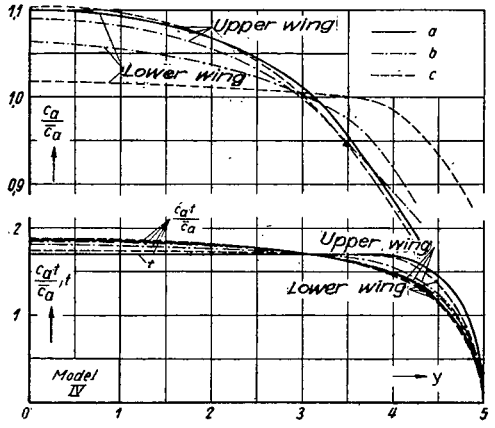

a- wings without interference;
b- wings with interference, unstaggered; c- wings with interference, staggered.

Figure 28.- Lift distributions.

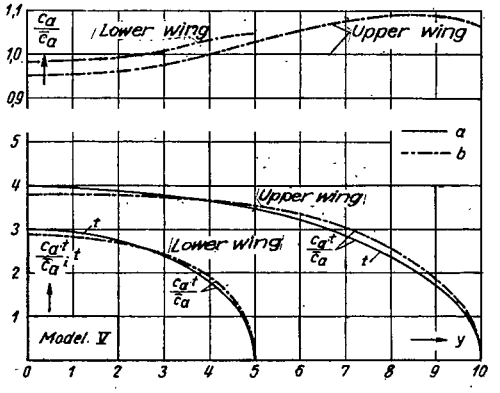

a- wings without interference;
b- wings with interference.

Figure 29.- Lift distributions.

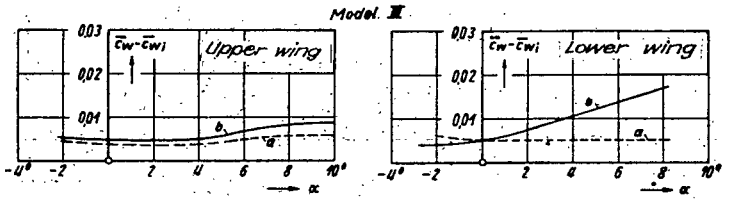

a- wings without interference;
b- wings with interference.

Figure 30.- Profile drag of wings.